Journal Name

RSC**Publishing**

ARTICLE

A Photo-tunable Membrane Based on Inter-particle Crosslinking for Decreasing Diffusion Rates

Song Li[a], Basem A. Moosa[a], Ye Chen[a], Wengang Li[a] and Niveen M. Khashab[a]

Functional polymeric membranes are widely used to adjust and control the diffusion of molecules. Herein, photosensitive poly(hydroxycinnamic acid) (PHCA) microspheres, which were fabricated by emulsification solvent-evaporation method, were embedded into ethyl cellulose matrix to fabricate composite membranes with a photo-tunable property. The photoreaction of PHCA is based on the [2+2] cycloaddition of cinnamic moieties upon irradiation with 365 nm light. Intra-particle crosslinking in PHCA microspheres was confirmed in the solution phase, while inter-particle crosslinking between adjacent PHCA microspheres dominated the solid membrane phase. The inter-particle crosslinking turned down the permeability of the composite membranes by 74%. To prove the applicability of the designed system, the composite membrane was coated on a model drug reservoir tablet. Upon irradiation of the tablet with UV light, the original permeability decreased by 57% and consequently the diffusion rate of the cargo (Rhodamine B) from the tablet slowed down. Most importantly, the tablet showed sustained release for over 10 days. This controllability can be further tuned by adjusting membrane thickness. The composite membranes showed excellent processing reproducibility together with consistent mechanical properties. These results demonstrate that incorporation of photosensitive PHCA microspheres in polymeric membranes provides a promising photo-tunable material for different applications including coating and separation.

Introduction

Polymeric membranes are widely used in various industries to provide support or separation and coating abilities.[1-4] Functional membrane materials have been applied in different dosage forms or devices, such as capsules,[5,6] tablets,[7,8] or implants,[9,10] to achieve desired bioactive functions including controlled or sustained release, taste masking, protection of unstable components, organ targeting, and antimicrobial or immune biofunctions. All these functions are based on the delicate control of membrane permeability,[11] which is impacted by the composition of intact membranes and their response to certain stimuli.

Desired diffusion processes can be controlled by conventional stimuli such as heat,[12,13] magnetic field[14,15] or pH change,[16-18] and an emerging number of systems are applying light to directly tune the diffusion behavior of solutes through coatings or membranes.[19-23] Light irradiation is preferentially chosen since it is environmentally friendly and inexpensive.[24-26] In photosensitive systems, bond degradation or change in chemical structure of chromophores always accompanies the photoreaction. Thus, the release or diffusion of payload can be tuned under proper irradiation. Reported photosensitive systems can have either indirect (energy transistors) or direct (chromophores) photo-behavior.[27] In the former systems, light energy is absorbed and transited to other stimuli by the transistor components, activating other stimuli-responsive behaviors. Some efficient energy transistors, such as gold nanoparticles[28,29] or carbon nanotubes[30,31] transiting light to heat and trigger thermosensitivity, are frequently utilized to obtain indirect photothermal behavior. However, the utilization of these transistors raised toxic risk to biological systems by potentially accumulating inorganic materials. On the other hand, in the direct systems, the photosensitivity is achieved through photoreactions of various chromophores, such as isomerization of azobenzene,[32,33] dimerization of anthracene,[34,35] or cleavage of o-nitrobenzylether.[19,36] Using synthetic chromophores also suffers from the drawback of low biocompatibility and high toxicity as most systems contain benzene and highly reactive moieties such as azo groups.

Among the classical photosensitive moieties, cinnamoyl or coumarin derivatives have been widely utilized in light-controlled systems.[37-39] Their photoreactions, which are based on the [2+2] cycloaddition between conjugated C=C double bonds under $\lambda > 280$nm irradiation (Figure S1), provide potential methods to introduce new crosslinks of different components. The formed crosslinks can therefore be utilized to modify the morphology or permeability of agent delivery systems, leading to controlled release. The natural make-up of these derivatives, existing greatly in plants such as cinnamon and storax,[40,41] makes them biologically superior to synthetic chromophores.

Journal of Materials Chemistry B Accepted Manuscript
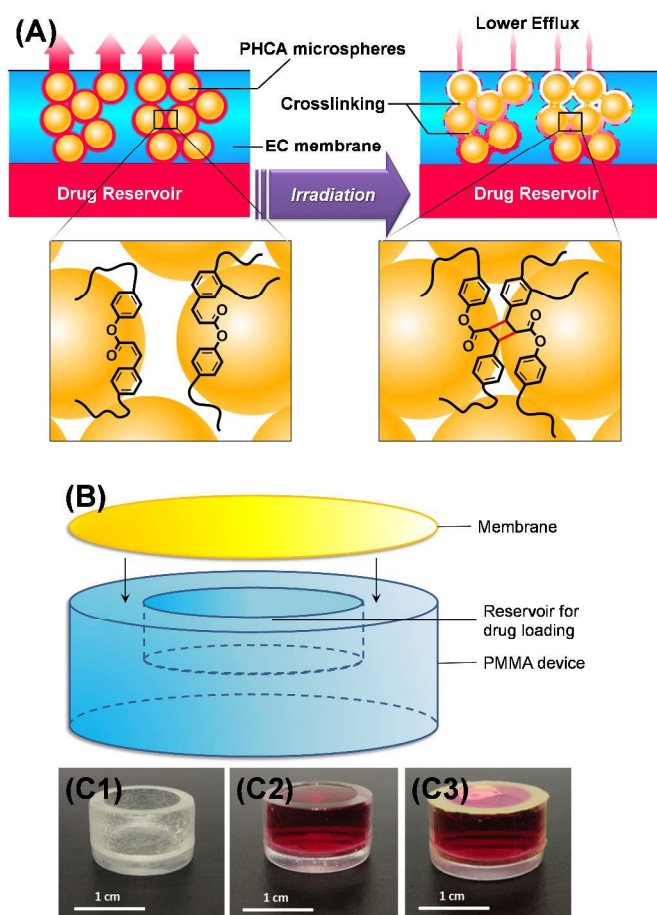
Figure 1. (A) Schematic illustration of photo-tunable "Turn down" of diffusion through composite membrane based on inter-particle crosslinking. (B) Schematic design of model reservoir tablets. Photographs show empty tablets (C1), tablets loaded with RhodamineB (RhB) solution (C2), and RhB loaded tablets coated with composite membrane (C3).

In this work, a polymeric membrane was designed and fabricated where the diffusion rate can be tuned by UV light irradiation (365 nm). Unlike most controlled delivery systems where stimuli are applied to trigger release or "on" state,[21, 22, 42, 43] our design significantly slowed down the release. For certain applications, such as coating or separation, an effective membrane is needed to have a permeability that can be turned down as desired. This design was later tested by coating a rhodamineB (RhB)-loaded model drug tablet (Figure 1). The photosensitive polymer used in the membrane, poly(hydroxycinnamic acid) (PHCA), was synthesized by thermal polycondensation of two hydroxycinnamoyl acids.[44] It was incorporated into ethyl cellulose (EC) membranes in the form of microspheres. Our design showed that the permeability of composite membranes could be turned down based on the crosslinking of microspheres upon UV light irradiation, which provided a light-tunable diffusion decrease over a long period of time. The results suggest the photosensitive composite membranes are promising candidates for application in sustained release formulations.

Experimental section

Materials

4-hydroxycinnamic acid (4-HCA), 3,4-dihydroxycinnamic acid (DHCA), and ethyl cellulose (EC, viscosity 46cP, 48% ethoxyl labeling extent) were purchased from Sigma Aldrich, USA. Sodium acetate anhydrous was purchased from Fisher Scientific, USA. Polyvinyl alcohol (PVA, Mw = 65000 g/mol) was purchased from Techno Pharmchem, India. Rhodamine B (RhB) was purchased from Alfa Aesar, USA. Phosphate buffer solution (PBS, pH=7.4), acetic anhydride, ethanol (98%), dichloromethane (DCM) and all other solvents of analytical grade were purchased from Fisher Scientific, USA.

Synthesis of photosensitive copolymer PHCA

Photosensitive copolymer PHCA was synthesized with a thermal polycondensation of 4-HCA and DHCA (Figure S2).[44, 45] Typically, the reaction took place in a three-necked round-bottomed flask where 4-HCA (10 mmol) and DHCA (10 mmol) were mixed into 10 ml acetic anhydride (condensation reagent) with trace amount of sodium acetate (catalyst). After alternate purging with nitrogen and vacuum three times, the temperature was increased to 190 °C under vacuum. At this temperature the reaction mixture became a clear solution, and this temperature was maintained for around 1h to remove almost all the solvent. Then the reaction was heated to 200 °C and maintained for another 3h to obtain melted product. The resulting mixture was dissolved into 20 ml dichloromethane (DCM) and precipitated in 200 ml acetone to remove the undissolved components. The supernatant was concentrated and precipitated with ethanol to obtain the polymer. PHCA was collected and dried in vacuum oven overnight.

The molecular weight of PHCA was measured by gel permeation chromatography (GPC, Agilent 1200 series), and the quantification of PHCA in DCM was achieved by UV/Vis spectroscopy. To examine the photoreaction of PHCA, a DCM solution containing about 0.01 mg/ml polymer was irradiated under 365nm UV beam from a longwave UV lamp (Blak-Ray® B-100AP/R high-intensity UV lamp, UVP Company, USA). The distance between solution and lamp was 10 cm (<20 mW/cm^2). The conditions of lamp and distance were kept constant for all the irradiation processes in this work. The absorption spectra of solution were then recorded by a UV/Vis spectrophotometer before and during irradiation period. Moreover, ^{1}H NMR spectrum (500 MHz Avance III, Bruker corporation, USA, using TMS as internal standard) were recorded in DCM-d$_2$ (CD$_2$Cl$_2$) before and after the polymer was irradiated in solution state. The PHCA solid was also irradiated directly in the same condition, followed by dissolving it in DCM to observe the change of its solubility.

Preparation of PHCA/PVA microspheres

PHCA/PVA microspheres were fabricated based on a conventional emulsification solvent-evaporation method.[46] DCM (4 ml) solution containing copolymer (40 mg/ml) was mixed with 25 ml deionized water containing 0.3% (w/v) PVA. After obtaining the emulsions under mechanical stirring (T25 digital ULTRA-TVRRAX, IKA, Germany) at 6000 rpm for 30 min, magnetic stirring was kept at 1000 rpm under atmospheric

condition overnight to evaporate organic solvent. On the second day the suspensions were centrifuged at 14000 rpm for 3min and supernatants were removed. The solids were washed with the same volume of deionized water, and then lyophilized to obtain microspheres powders.

PHCA and PVA composition in the obtained PHCA/PVA microspheres was determined by measuring PHCA content with UV/Vis spectroscopy after dissolving 10 mg microspheres into DCM after sonication. The photo-behavior of PHCA/PVA microspheres, which was either agglomeration or shrinkage of particles, was observed by triggering crosslinking under 365nm light. The morphological change of microspheres after irradiation was observed by transmission electron microscopy (TEM Tecnai T12, FEI, USA) and then further verified by dynamic light scattering (NanoZS Zetasizer, Malvern, UK). Microspheres of three concentrations were irradiated: (A) Low concentration (20 µg/ml) of microspheres dispersed in water; 7 dispersion samples of the same batch were irradiated separately for 0, 1, 2, 3, 4, 6 or 24 hours. (B) Medium concentration (1×10^3 µg/ml) of microspheres dispersed in water; 7 dispersion samples of the same batch were irradiated following the same procedure. (C) High concentration (4×10^4 µg/ml) of microspheres dispersed in water, and then allowed to dry on a glass slide (solid phase). With control groups of 7 samples for each state set without any irradiations but following the same procedure of size measurement, the change of average particle sizes can act as a clear indication of either agglomeration or shrinkage.

Fabrication of composite membrane

A casting method was utilized to fabricate the composite membranes doped with photosensitive microspheres. As matrix material, EC was dissolved into ethanol to 10% (w/w) concentration. The obtained solution was mixed with the desired amount of PHCA/PVA microspheres (the doping ratio was 100 mg microspheres in 100 mg EC matrix) to generate a casting solution which was then casted on glass slides by a stainless casting blade (1117 micrometer adjustable film applicator, Sheen Instruments, UK, original blade height was set at 300 µm). The obtained membranes (EC/PHCA/PVA membrane) were allowed to dry at room temperature overnight before being collected in water bath. Membranes with different thicknesses were fabricated in the same way by alternating the original blade height to 150 µm, 300 µm or 450 µm.

As controls, two kinds of membranes without PHCA were fabricated: EC and EC/PVA membranes. Generally, EC membranes contain only EC matrix without any doping, and they were used in demonstrating the behavior and influence of microspheres in EC matrix. These membranes were casted directly with 10% (w/w) EC in ethanol solution. While EC/PVA membranes contain the corresponding content of PVA but without PHCA, they were used for demonstrating the influence of photoreactions on the permeability of membranes. To cast these membranes, 2% PVA aqueous solution was first mixed with ethanol at ratio of 20:80 to obtain homogeneous colorless solution, followed by dissolving EC to 10% (w/w) concentration for casting.

Scanning electron microscopy (SEM Quanta 600, FEI, USA) was utilized to observe the cross-section of all membranes. Using SEM, their thickness was also measured as a mean value from at least 8 different positions along the cross-sections. To verify the crosslinks formed in the membranes, thermal mechanical properties were studied with dynamic mechanical analysis (DMA) on DMA 242C (Netzsch, Germany). Tests were performed in the tension mode at a constant frequency of 1 Hz, with the static force at 0.3 N and the dynamic force at 0.2 N, in the temperature range of 30 to 180 °C with the heating rate of 2 °C/min. The diffusion tests were performed in side-by-side diffusion cells (PermeGear, Inc., USA) after all membrane samples were hydrolyzed in water bath for above 1h. In the donor chamber, 1 mg/ml RhB was loaded as the cargo in the tablet's reservoir, while deionized water (receptor medium) was filled in the other side. The temperature of both chambers was controlled at 37°C. At predicted time points samples were collected from the receptor chamber to analyze the RhB concentration by UV/Vis spectroscopy at 554nm, and then restored to continue the diffusion tests.

Solute permeability was calculated using equation (1) based on Fick's first law of diffusion with several assumptions including: (a) the permeation area on the membrane, S, and the drug concentration in the donor chamber, C_d, can be considered as constant; (b) sink condition is maintained in the receptor chamber during diffusion process; (c) a steady diffusion state is reached after a lag time t_L.[47, 48]

$$M_t = P \cdot S \cdot C_d \cdot (t - t_L) \tag{1}$$

Here M_t is the mass transport through membrane till time t. By this equation the permeability (P) was calculated from the slope of M_t - t curve at the steady state. The relative permeability ($P_{relative}$) was also calculated using equation (2). By comparison of permeability before (control) and after irradiation (UV), $P_{relative}$ could be used to describe the photosensitive controllability: a $P_{relative}$ further away from value 1 indicated a bigger difference after stimuli and thus better controllability.

$$P_{relative} = P_{UV} / P_{control} \tag{2}$$

Fabrication of RhB-loaded reservoir tablets

To better observe the practical diffusion controllability of the composite membranes, tablets (Figure 1) were designed and fabricated to simulate diffusion from reservoir devices such as microchips or insoluble matrix pills. A small chamber (Φ 10 mm, 6 mm depth) was drilled on the poly(methyl methacrylate) (PMMA) tablet as container to load RhB solution (1 mg/ml in pH 7.4 PBS). Composite membranes (casted with 300 µm original blade setting) were then adhered to the upper surface by polydimethylsiloxane (PDMS) to cover the drug chamber after they were activated by irradiation. The model reservoir tablets were stored for two days under room temperature with constant humidity to allow the drying of PDMS adhesion. The release tests were performed in 40ml pH 7.4 PBS at 37°C, irritated in a shaker at 100 rpm. At predicted time, solution samples were collected to measure the amount of RhB released from reservoir tablets, and the whole release tests were continued over 10 days.

Statistical analysis

The one-tailed Student's t-test was used to compare all data. All results are presented as means ± S.D., and difference of $p < 0.05$ was considered statistically significant.

Results and discussion

Synthesis and photoreaction of PHCA

The molecular weight of PHCA was 5.79×10^3 g/mol (Mw) (PDI=2.23) as measured by GPC, and the structure of polymer was verified by 1H NMR (Figure 2A). The photoreaction of PHCA is based on the [2+2] cycloaddition between cinnamic moieties, where the conjugated C=C double bonds are consumed to generate cyclobutane structure among polymer chains. Clear changes were seen in the NMR spectrum of PHCA after UV light irradiation (Figure 2B). While the intensity of double bonds (peak a, b) decreased, several new peaks at $\delta = 3.5 \sim 5$ ppm (which are characteristic of cyclobutane) were obtained, indicating that the polymer chains were crosslinked by [2+2] cycloaddition.

Since the conjugated C=C double bonds were consumed during the photoreaction, which could significantly decrease the level of unsaturation, the formation of cyclobutane crosslinks can be also monitored from UV/Vis spectrum where the absorbance of PHCA is decreased.[49-51] As shown in Figure 3, PHCA had clear absorbance peak near 300nm wavelength, and this peak gradually decreased over 20 hours of UV irradiation time, supporting the photoreaction between cinnamic moieties in PHCA. From the decrease of absorption, it could be calculated as 69.7% of cinnamic moieties consumed in current experimental condition. Moreover, if PHCA was irradiated in solid state, its solubility was significantly decreased. While original PHCA could well dissolve in DCM, the highly crosslinked PHCA could not completely dissolve (Figure S3). Unlike polymers that are irradiated in solution state, PHCA chains in solid condition are packed closely generating the undissolved product after irradiation.
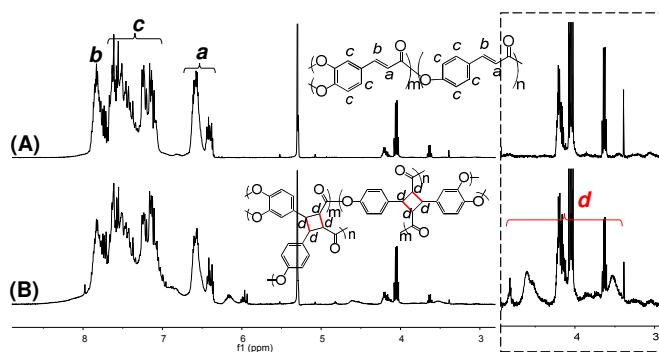
Figure 2. ¹H NMR spectrum of PHCA before (A) and after (B) UV irradiation. (~5mg/ml PHCA in DCM-d₂) The dashed inserts are magnification of corresponding spectrum in area 3~5 ppm, showing generated peaks of cyclobutane along polymer chains.
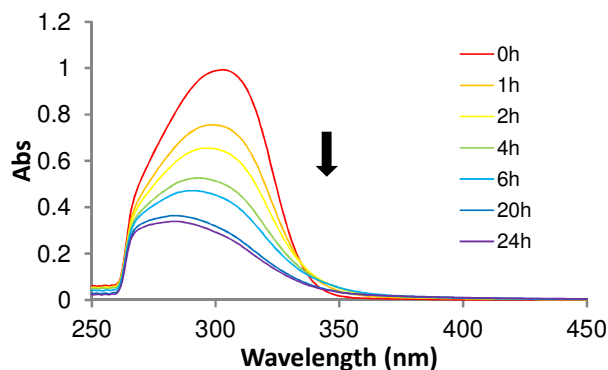
Figure 3. Absorbance decrease of PHCA (~10µg/ml in DCM) under 365nm irradiation at different durations.

Composition, photo-behavior and morphology of microspheres

The absorbance peak at 300nm was used to quantify PHCA by UV/Vis spectroscopy (Figure S4). The composition of PHCA was measured by determining the PHCA contents in 10mg microspheres, which was 90.47 ± 1.80% (w/w) in the obtained microspheres. This indicated that around 9.53% (w/w) was PVA.

The photo-triggered cycloaddition among PHCA chains could happen in either solution or dry states. Since PHCA consisted of whole cinnamate groups along all the backbones and branches, it could be cross-linked in relatively high degree, influencing the morphology of microspheres consisting of PHCA. The agglomeration caused by crosslinking can be easily observed by TEM images of microspheres before and after irradiation (Figure 4). Most particles agglomerated and fused with each other after 365nm light treatment, losing their clear boundaries before irradiation.

To further study these morphological changes, an average size measurement of microspheres was performed. Even with a broad size distribution, the continuous change still provided a clear indication of what process (inter- or intra-particle crosslinking) was taking place. It has been reported that nanoparticles made of this photosensitive polymer show significant shrinkage following photoreactions in solution.[52] Similar results were obtained by UV irradiation of our synthesized PHCA/PVA spheres in solution. That is, when microspheres were irradiated at a relatively low concentration (20 µg/ml), the average size decreased clearly (Figure S5A) due to the increased intra-particle crosslinking degree of polymers within the spheres.[52, 53] After 2h irradiation the particle size began to decline and the final average size decrease was about 50% after 24h. In this relatively diluted state, the distance between microspheres is big enough to prevent their contact and thus to prevent inter-particle crosslinking. The size change was limited when microspheres of a relatively higher concentration (1000 µg/ml) were irradiated (Figure S5B). In this denser dispersion, the microspheres can contact each other much more easily so a competition between intra- and inter-particle interactions takes place leading to minimal effect on the overall size. To support this assumption, an extremely high concentration (4×10^4 µg/ml) of microspheres was utilized for the same test. The particles were dried on a glass slide to give a

much denser dry state before direct irradiation. The size gradually grew to about 300% the original value (Figure S5C), indicating the agglomeration of particles. For comparison, all control groups without irradiation generally maintained their original size. In the dry state with higher concentration, most microspheres are in contact with each other, and thus inter-particle crosslinking was believed to occur more easily and thus dominated over the competing intra-particle interaction. As a result a significant size increase of particles, which was caused mainly by the agglomeration of microspheres, was observed.
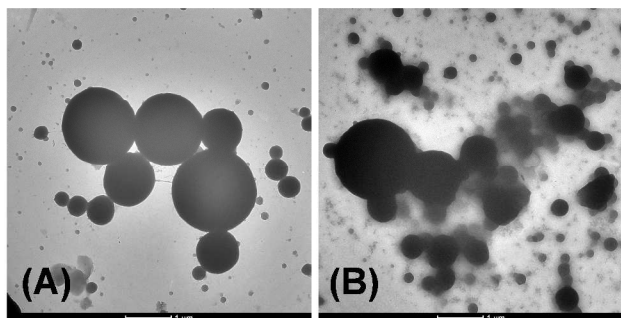

Figure 4. TEM images of microspheres (1mg/ml in water dispersion) before (A) and after (B) 365nm irradiation, indicating the particles agglomerated after irradiation. The scale bar indicates 1 µm.

Morphology of composite membranes

Incorporation of either PVA or PHCA/PVA microspheres into EC matrix could significantly change the appearance of the membranes (Figure S6). Pure EC typically formed obscure or semi-transparent membranes with smooth surface. The membrane turned to be turbid and white with a rough surface when PVA was mixed into EC. Doping with PHCA/PVA microspheres generated a yellowish membrane, which originates from PHCA. Compared to EC/PVA, EC/PHCA/PVA membrane was closer to EC with an obscure rather than turbid appearance.

Due to the extra space occupied by either microspheres in EC/PHCA/PVA membranes or pores in EC/PVA ones, their film thickness, 25.63 ± 2.37 µm and 28.59 ± 0.36 µm respectively, was higher than that of pure EC membranes (Table S1). Meanwhile, for the composite membranes themselves, the thickness was tunable by varying the original blade height; elevating the casting blade leaded to thicker membranes. From 150 µm original setting which resulted in thickness of 10.79 ± 1.44 µm, the film thickness increased by around 12~15 µm when the casting blade was elevated by 150 µm each time.
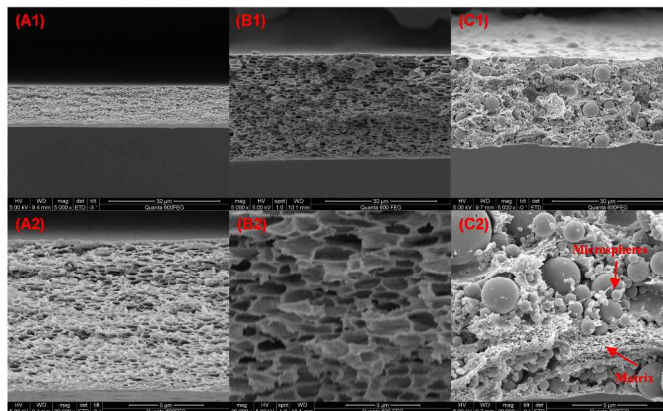

Figure 5. SEM images of the cross-section of EC (A1, A2), EC/PVA (B1, B2) and EC/PHCA/PVA (C1, C2) membranes. Images A2, B2, C2 (scale bar = 5 µm) are magnification of A1, B1, C1 (scale bar = 30 µm), respectively. Arrows in C2 indicate the microspheres and EC matrix.

SEM images showed that the internal structure of membranes was greatly changed when PVA or microspheres were incorporated. While the pure EC membrane showed relatively dense sponge-like cross-section (Figure 5, A1 and A2), a more porous honeycomb-like structure appeared in EC/PVA membrane (Figure 5, B1 and B2) whose preparation included incorporation of aqueous contents. It is well known that due to the slower evaporation rate than ethanol, moisture in casting solution introduces a significant pore-forming phenomenon.[54, 55] The slight sponge-like structure in pure EC films can be attributed to the moisture in ethanol. When PVA with aqueous contents were incorporated during fabrication, the pores formed in membranes were even bigger, and the resulting EC/PVA membranes were highly porous. The more porous internal structure in the EC/PVA films also caused the turbid appearance of EC/PVA membranes. On the other hand, incorporation of PHCA/PVA microspheres did not introduce significant moisture evaporation, and these microspheres were dispersed in casting solution. Since the microspheres were not soluble in ethanol, they maintained their sphere structure during the whole fabrication process (Figure 5, C1 and C2). Therefore, the cross-section of EC/PHCA/PVA membrane showed the PHCA microspheres simply embedded in EC matrix. Interestingly the PHCA had fluorescence under irradiation (λ_{Ex} = 354nm, λ_{Em} = 456nm, Figure S7), this provided an opportunity to observe microspheres from the top view of membranes (Figure S8) by confocal laser scanning microscopy (CLSM). Confocal images showed that the microspheres were packed very close in the composite membrane so as to allow inter-particle crosslinking.

Thermal mechanical properties of composite membrane

The light-induced crosslinking in composite membranes was further verified by characterizing the mechanical properties of these films with DMA. Figure 6A shows the storage modulus of membranes with or without UV irradiation (temperature ranged from 50 to 170 °C). Compared with EC membranes, EC/PHCA/PVA composite membranes presented lower modulus indicating poorer mechanical properties. This is reasonable since the incorporation of microspheres introduced porous or deficient structures in the membrane, which made the

films more brittle. Two relaxation stages existed in the composite membrane, which could be attributed to the two components in film materials. It was noted, however, that the storage modulus was restored significantly after membrane was irradiated by UV light, and thus the modulus at 110 °C increased by 1.7 times, from 573 MPa to 987 MPa. The formation of crosslinks in the irradiated membrane strengthened its mechanical properties.[56, 57]
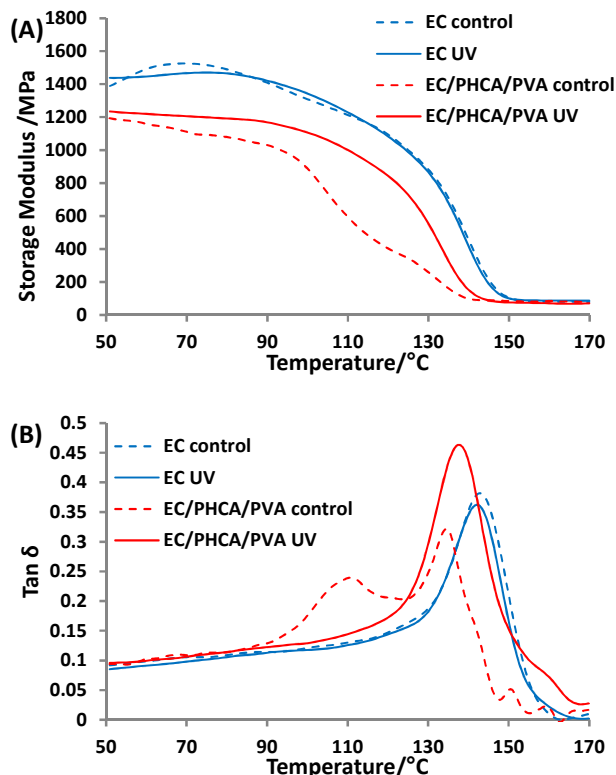
Figure 6. Storage modulus (A) and Tan δ (B) curves versus temperature for the EC or EC/PHCA/PVA membrane without (control) or with (UV) 365nm irradiation.

Correspondingly, Tan δ (loss modulus/storage modulus) of these membranes was shown in Figure 6B, where the peaks represented the temperature at which the polymeric materials undertook the maximum change in mobility of polymer chains and network. EC films had only one peak around 142 °C in this figure, which was corresponding to the glass transition temperature (T_g) of EC.[58] EC/PHCA/PVA composite membrane had two separated Tan δ peaks at around 135 °C and 110 °C, respectively owning to behaviors of matrix and fillers,[59] indicating the true immiscibility of matrix and microsphere fillers.[60] This corresponded well to the two relaxation stages in the storage modulus curve. T_g of EC decreased to about 135 °C after microspheres were incorporated in the film[61-63] and the motion of PHCA chains is contributing to a second Tan δ peak at 110 °C. However, clear changes were observed after UV irradiation. First, the T_g of EC matrix increased to about 138 °C, meaning the local motion of polymer chains was limited after the formation of crosslinks among microspheres; second, the Tan δ peak of PHCA disappeared within current temperature range, indicating that the motion of PHCA chains was inhibited after being crosslinked and that the phase transition did not occur. In fact,

considering greater networks or agglomerates were formed during this crosslinking process, the phase transition of PHCA might happen at a higher temperature exceeding the tested range.[64-66]
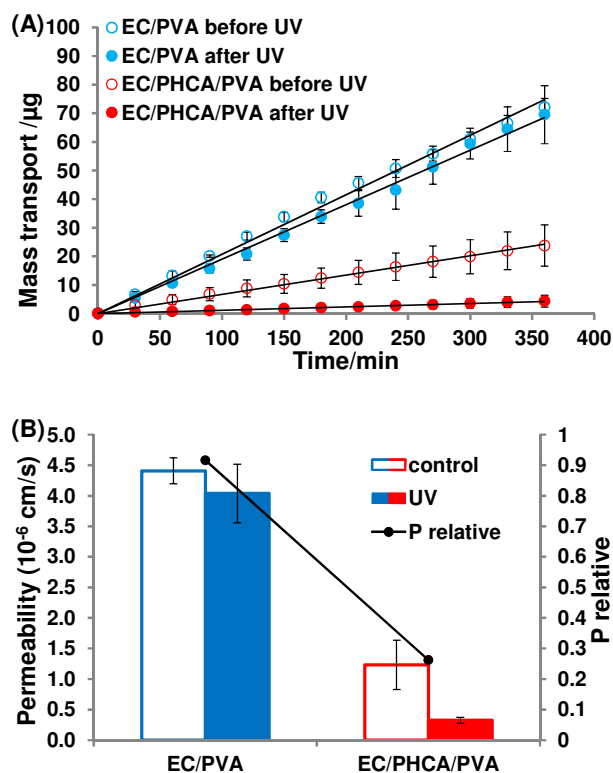

Figure 7. (A) Diffusion profiles of RhB through EC/PVA (blue) or EC/PHCA/PVA (red) membranes before (empty symbols, control group) or after (solid symbols, UV group) the membranes were given UV irradiation. RhB contents were measured by UV/Vis spectroscopy over time. (B) Permeability change of two types of membranes after irradiation. Permeability and $P_{relative}$ was calculated from the diffusion profiles according to Equation (1) and (2), respectively. All data was shown as mean ± SD, n=3.

Permeability of composite membranes

To verify the photosensitive operation of EC/PHCA/PVA membranes, diffusion tests were performed both before and after UV irradiation, and EC/PVA membranes were utilized in the same tests as controls. Compared to EC/PVA diffusion plots, EC/PHCA/PVA membranes showed much slower diffusion (before irradiation). While EC/PVA membranes diffused around 70 μg RhB during 6h, EC/PHCA/PVA had a diffusion of about 20 μg in the same period (Figure 7A). After irradiation, the diffusion through EC/PHCA/PVA films was slowed down to <10 μg, showing a significant declination in the permeability of photosensitive films. With the same treatment for the same period, EC/PVA membranes maintained almost unchanged diffusion. Moreover, the diffusion within 6h appeared to be zero-order since linear regression was achieved for all membranes (R^2>0.99). This suggested that no apparent lag time was observed during the current diffusion process.

This comparison indicated that the photosensitive diffusion change was attributed to the photoreaction of PHCA rather than PVA or EC matrix. A clear comparison of permeability of those membranes also suggested that only EC/PHCA/PVA membrane possessed the photosensitive controllability, and that its permeability significantly decreased from 1.23×10^{-6} cm/s to 3.23×10^{-7} cm/s (p=0.02) after treatment with UV light (Figure 7B). Meanwhile, the permeability change of EC/PVA membranes is not significant, from 4.40×10^{-6} cm/s to 4.03×10^{-6} cm/s (p=0.41). Compared to EC/PVA membrane of $P_{relative}$ >0.9, which showed no significant change of permeability, EC/PHCA/PVA membrane of $P_{relative}$ ≈0.26 had obvious photosensitive controllability, indicating about 74% decrease of permeability. The original diffusion route in photosensitive membranes is blocked by these generated inter-particle crosslinks, and thus the diffusion is slowed down by either longer penetration pathway or lower porosity of membrane. The diffusion behavior and controllability could also be tuned further by varying the thickness of casted films (Figure 8). Increasing thickness from 11 µm to 37 µm declined $P_{relative}$ value from 0.6 to 0.3, indicating that more tuning can be achieved utilizing thicker membranes. This is reasonable since more crosslinking could occur in thicker membranes, which consequently impacts the diffusion pathways and the overall porosity.
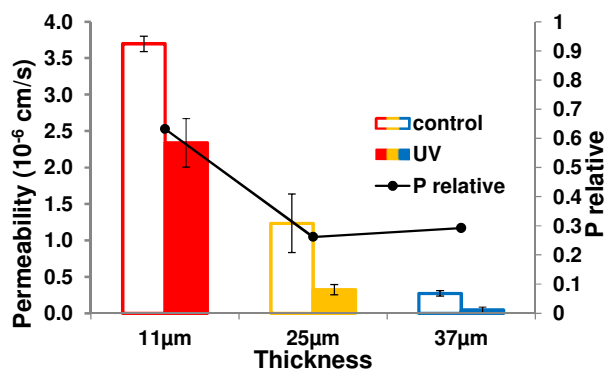

Figure 8. Permeability comparison of composite membranes with different thicknesses before (empty columns, control group) and after (solid columns, UV group) irradiation. Permeability and $P_{relative}$ was calculated from the diffusion profiles according to Equation (1) and (2), respectively. All data was shown as mean ± SD, n=3.

Release behavior of film-coated tablets

To validate the operation of composite membranes in practical diffusion conditions over a longer period of time, the films were coated on reservoir tablets to simulate a sustained release process. During 10 days of testing, these membranes maintained their photosensitive controllability when they were mounted on PMMA tablets (Figure 1). For tablets without irradiation, more than 70% of loaded RhB was released into buffer solution over 10 days, while those with irradiation released less than 30% of payloads, indicating that permeability declined by around 57% over this period (Figure 9). Compared to diffusion tests performed with diffusion cells, drug release from tablets into medium had two main differences: (i) while diffusion cells utilize 200 rpm stirring to better mix solutions in both donor and receptor chambers, no stirring existed in the

container of reservoir tablets; (ii) cargo concentration in donor chamber was no longer considered as constant. Therefore, the experimental design for testing release from model tablets is closer to the practices used in sustained drug delivery formulations. It may also be observed that the declination of permeability (~57%) was not as high as that in previous diffusion cell tests (~74%), and this might be attributed to the PDMS adhesion in small area of membranes. Considering the significant decrease of diffusion from tablets, the composite membrane maintained good controllability on the permeability for sustained diffusion or release.
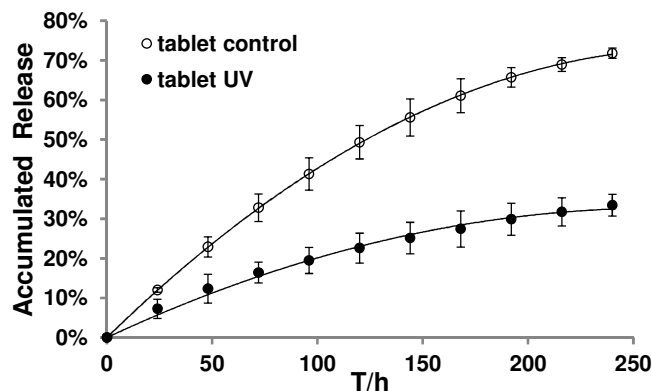
Figure 9. Release profile of RhB from PMMA tablets coated with composite membranes before (empty symbols, control group) and after (solid symbols, UV group) irradiation. The coating membranes had thickness of ~25µm. All data was shown as mean ± SD, n=3.

Conclusions

Photo-tunable composite membranes were designed and fabricated to control diffusion by UV irradiation. A photosensitive polymer, poly(hydroxycinnamic acid), was synthesized and incorporated into EC matrix in the form of light responsive (PHCA/PVA) microspheres. Spectroscopy and microscopy results showed that inter-particle crosslinking between highly compact spheres in the membrane after UV irradiation led to microspheres agglomeration and reduced membrane permeability. This photo-behavior was further verified by DMA as crosslinking improved the mechanical properties of composite membranes. Based on the crosslinking of microspheres, diffusion routes were blocked so as EC/PHCA/PVA composite membrane (in diffusion cell) had 74% decrease in the cargo release rate after irradiation, while this composite membrane on a tablet model showed a 57% decrease. Through easily controlling the membrane thickness, even further tuning can be achieved. Thus, depending on the amount of cargo that needs to be released, different membrane thickness can be used for coating. Moreover, varying the irradiation time could also provide more control as the maximum crosslinking occurred after 20h. Thus, if more permeability (less crosslinking) is needed the irradiation time can be shortened. Different materials can be easily coated with this photo-responsive polymeric membrane then UV irradiated to achieve the desired permeability for various applications. This affords a promising, cheap, and safe control over diffusion in delivery systems especially when prolonged and sustained release is preferred.

Acknowledgements

Notes and references

[a] Controlled Release and Delivery Laboratory (CRD), Center of Membrane and Porous Materials, King Abdullah University of Science and Technology (KAUST), Thuwal 23955-6900, Kingdom of Saudi Arabia. Tel: +966 012 8082410. E-mail: niveen.khashab@kaust.edu.sa.

† Electronic Supplementary Information (ESI) available: [Scheme of photoreaction and synthesis of PHCA, photographs of polymer solubility change after irradiation, quantification calibration of PHCA, size change of microspheres in three different state upon irradiation, photographs of composite membranes, thickness of membranes fabricated under different settings, fluorescence spectrum of PHCA and CSLM images of composite membrane]. See DOI: 10.1039/b000000x/

1. M. E. Tanaka, *Nature*, 2005, **437**, 656.
2. K. P. Lee, T. C. Arnot and D. Mattia, *J. Membr. Sci.*, 2011, **370**, 1-22.
3. R. Laga, R. Carlisle, M. Tangney, K. Ulbrich and L. W. Seymour, *J. Controlled Release*, 2012, **161**, 537-553.
4. M. E. Lynge, R. van der Westen, A. Postma and B. Staedler, *Nanoscale*, 2011, **3**, 4916-4928.
5. Y. Ma, W.-F. Dong, M. A. Hempenius, H. Moehwald and G. J. Vancso, *Nat. Mater.*, 2006, **5**, 724-729.
6. B. Thu, P. Bruheim, T. Espevik, O. Smidsroed, P. Soon-Shiong and G. Skjak-Braek, *Biomaterials*, 1996, **17**, 1031-1040.
7. T. Tokumura and Y. Machida, *J. Control. Release*, 2006, **110**, 581-586.
8. E. Fukui, K. Uemura and M. Kobayashi, *J. Control. Release*, 2000, **68**, 215-223.
9. C. Wang, B. Yu, B. Knudsen, J. Harmon, F. Moussy and Y. Moussy, *Biomacromolecules*, 2008, **9**, 561-567.
10. M. Stigter, J. Bezemer, K. de Groot and P. Layrolle, *J. Controlled Release*, 2004, **99**, 127-137.
11. R. Bodmeier, *Eur. J. Pharm. Biopharm.*, 1997, **43**, 1-8.
12. Y. Chen, A. Bose and G. D. Bothun, *ACS Nano*, 2010, **4**, 3215-3221.
13. Q. Fan, K. K. Sirkar and J. Wu, *J. Membr. Sci.*, 2009, **337**, 175-181.
14. T. Hoare, B. P. Timko, J. Santamaria, G. F. Goya, S. Irusta, S. Lau, C. F. Stefanescu, D. Lin, R. Langer and D. S. Kohane, *Nano Lett.*, 2011, **11**, 1395-1400.
15. I. Savva, A. D. Odysseos, L. Evaggelou, O. Marinica, E. Vasile, L. Vekas, Y. Sarigiannis and T. Krasia-Christoforou, *Biomacromolecules*, 2013, **14**, 4436-4446.
16. J. Du, Y. Tang, A. L. Lewis and S. P. Armes, *J. Am. Chem. Soc.*, 2005, **127**, 17982-17983.
17. G. Zhai, L. Ying, E. T. Kang and K. G. Neoh, *Macromolecules*, 2002, **35**, 9653-9656.
18. L. Ying, P. Wang, E. T. Kang and K. G. Neoh, *Macromolecules*, 2002, **35**, 673-679.
19. N. Fomina, C. McFearin, M. Sermsakdi, O. Edigin and A. Almutairi, *J. Am. Chem. Soc.*, 2010, **132**, 9540-9542.
20. K. Sumaru, K. Ohi, T. Takagi, T. Kanamori and T. Shinbo, *Langmuir*, 2006, **22**, 4353-4356.
21. W.-C. Jeong, S.-H. Kim and S.-M. Yang, *ACS Applied Materials & Interfaces*, 2014, **6**, 826-832.
22. E. G. Randles and P. R. Bergethon, *Langmuir*, 2013, **29**, 1490-1497.
23. Q. Jin, F. Mitschang and S. Agarwal, *Biomacromolecules*, 2011, **12**, 3684-3691.
24. I. Tomatsu, K. Peng and A. Kros, *Adv Drug Deliv Rev*, 2011, **63**, 1257-1266.
25. B. P. Timko, T. Dvir and D. S. Kohane, *Adv. Mater.*, 2010, **22**, 4925-4943.
26. D. Habault, H. Zhang and Y. Zhao, *Chem. Soc. Rev.*, 2013, **42**, 7244-7256.
27. S. Li, W. Li and M. Khashab Niveen, in *Nanotechnology Reviews*, 2012, vol. 1, p. 493.
28. A. Wijaya and K. Hamad-Schifferli, *Langmuir*, 2008, **24**, 9966-9969.
29. M. S. Yavuz, Y. Cheng, J. Chen, C. M. Cobley, Q. Zhang, M. Rycenga, J. Xie, C. Kim, K. H. Song, A. G. Schwartz, L. V. Wang and Y. Xia, *Nature materials*, 2009, **8**, 935-939.
30. K. Welsher, Z. Liu, D. Daranciang and H. Dai, *Nano Lett.*, 2008, **8**, 586-590.
31. N. W. S. Kam, M. O'Connell, J. A. Wisdom and H. Dai, *Proc. Natl. Acad. Sci. U. S. A.*, 2005, **102**, 11600-11605.
32. X. Liao, G. Chen, X. Liu, W. Chen, F. Chen and M. Jiang, *Angew. Chem. Int. Ed.*, 2010, **49**, 4409-4413.
33. C. Raimondo, F. Reinders, U. Soydaner, M. Mayor and P. Samori, *ChCom*, 2010, **46**, 1147-1149.
34. Y. Zheng, M. Micic, S. V. Mello, M. Mabrouki, F. M. Andreopoulos, V. Konka, S. M. Pham and R. M. Leblanc, *Macromolecules*, 2002, **35**, 5228-5234.
35. Y. Sako and Y. Takaguchi, *Org. Biomol. Chem.*, 2008, **6**, 3843-3847.
36. J. Cao, S. Huang, Y. Chen, S. Li, X. Li, D. Deng, Z. Qian, L. Tang and Y. Gu, *Biomaterials*, 2013, **34**, 6272-6283.
37. J. Ling, M. Z. Rong and M. Q. Zhang, *JMCh*, 2011, **21**, 18373-18380.
38. M. Nagata and Y. Yamamoto, *React. Funct. Polym.*, 2008, **68**, 915-921.
39. J. Babin, M. Pelletier, M. Lepage, J.-F. Allard, D. Morris and Y. Zhao, *Angew. Chem. Int. Ed.*, 2009, **48**, 3329-3332.
40. W. Boerjan, J. Ralph and M. Baucher, *Annu. Rev. Plant Biol.*, 2003, **54**, 519-546.
41. D. Hernanz, V. Nuñez, A. I. Sancho, C. B. Faulds, G. Williamson, B. Bartolomé and C. Gómez-Cordovés, *J. Agric. Food Chem.*, 2001, **49**, 4884-4888.
42. X. An, F. Zhan and Y. Zhu, *Langmuir*, 2013, **29**, 1061-1068.
43. A. Pashkovskaya, E. Kotova, Y. Zorlu, F. Dumoulin, V. Ahsen, I. Agapov and Y. Antonenko, *Langmuir*, 2010, **26**, 5726-5733.
44. T. Kaneko, T. H. Thi, D. J. Shi and M. Akashi, *Nature materials*, 2006, **5**, 966-970.
45. M. Matsusaki, A. Kishida, N. Stainton, C. W. G. Ansell and M. Akashi, *J. Appl. Polym. Sci.*, 2001, **82**, 2357-2364.
46. K. Khaled, H. Sarhan, M. Ibrahim, A. Ali and Y. Naguib, *AAPS PharmSciTech*, 2010, **11**, 859-869.
47. J. Siepmann, R. Siegel and F. Siepmann, in *Fundamentals and Applications of Controlled Release Drug Delivery*, eds. J. Siepmann, R. A. Siegel and M. J. Rathbone, Springer US, 2012, ch. 6, pp. 127-152.
48. K. Zhang and X. Y. Wu, *Biomaterials*, 2004, **25**, 5281-5291.
49. Y. Chen and K.-H. Chen, *Journal of Polymer Science, Part A: Polymer Chemistry*, 1997, **35**, 613-624.
50. S. R. Trenor, A. R. Shultz, B. J. Love and T. E. Long, *Chem. Rev.*, 2004, **104**, 3059-3078.

51. J. Jiang, B. Qi, M. Lepage and Y. Zhao, *Macromolecules*, 2007, **40**, 790-792.
52. D. Shi, M. Matsusaki, T. Kaneko and M. Akashi, *Macromolecules*, 2008, **41**, 8167-8172.
53. D. Shi, T. Kaneko and M. Akashi, *Langmuir*, 2007, **23**, 3485-3488.
54. S. Narisawa, H. Yoshino, Y. Hirakawa and K. Noda, *Chem. Pharm. Bull. (Tokyo)*, 1993, **41**, 329-334.
55. E. Chevalier, D. Chulia, C. Pouget and M. Viana, *J. Pharm. Sci.*, 2007, **97**, 1135-1154.
56. R. Polanský, M. Pinkerová, M. Bartunková and P. Prosr, *Journal of Electrical Engineering*, 2013, **64**, 361-365.
57. V. Litvinov and A. Dias, *Macromolecules*, 2001, **34**, 4051-4060.
58. W. He, Y. Du and L. Fan, *J. Appl. Polym. Sci.*, 2006, **100**, 1932-1939.
59. J.-S. Park, J.-W. Park and E. Ruckenstein, *Polymer*, 2001, **42**, 4271-4280.
60. T. M. Nair, M. G. Kumaran, G. Unnikrishnan and V. B. Pillai, *J. Appl. Polym. Sci.*, 2009, **112**, 72-81.
61. H. Ishida and Y.-H. Lee, *Polymer*, 2001, **42**, 6971-6979.
62. C. Xiang, P. J. Cox, A. Kukovecz, B. Genorio, D. P. Hashim, Z. Yan, Z. Peng, C.-C. Hwang, G. Ruan, E. L. G. Samuel, P. M. Sudeep, Z. Konya, R. Vajtai, P. M. Ajayan and J. M. Tour, *ACS Nano*, 2013, **7**, 10380-10386.
63. H. Xia and M. Song, *Soft Matter*, 2005, **1**, 386-394.
64. D. J. Sessa, A. Mohamed and J. A. Byars, *J. Agric. Food Chem.*, 2008, **56**, 7067-7075.
65. B. Wang, N. Hong, Y. Shi, B. Wang, H. Sheng, L. Song, Q. Tang and Y. Hu, *Radiat. Phys. Chem.*, 2014, **97**, 284-291.
66. G. W. Selling and K. D. Utt, *J. Appl. Polym. Sci.*, 2014, **131**, 40122.

Photo-tunable "Turn down" of Diffusion Based on A Photo-tunable Membrane Based on Inter-particle Crosslinking for Decreasing Diffusion Rates

Song Li[a], Basem A. Moosa[a], Ye Chen[a], Wengang Li[a] and Niveen M. Khashab[a]

1